MOLECULAR PHYSICS, 10 JUNE 2003, VOL. 101, NO. 11, 1705–1711

Taylor & Francis
Taylor & Francis Group

The polarization energy of normal liquid ^{3}He

F. H. ZONG[1], D. M. CEPERLEY[1]*, S. MORONI[2] and S. FANTONI[3]

[1]Department of Physics and NCSA, University of Illinois at Urbana-Champaign, Urbana, IL 61801, USA
[2]INFM Center for Statistical Mechanics and Complexity, Department of Physics, Universitá di Roma 'La Sapienza', Rome, Italy
[3]SISSA and INFM DEMOCRITOS National Simulation Center, Trieste, Italy

(*Received 1 November 2002; accepted 2 December 2002*)

We present new quantum Monte Carlo calculations of the ground-state energy of liquid ^{3}He using backflow and 3-body wavefunctions and twist-averaged boundary conditions. We estimate the effects of the 3-body potential and compare to experimental measurements of the unpolarized equation of state and the magnetic susceptibility. There is still a large discrepancy with respect to the magnetic susceptibility, requiring either improved nodal surfaces or going beyond the fixed-node method.

1. Introduction

The calculation of the ground-state energy of liquid ^{3}He is an important benchmark for the progress of microscopic theory. The most successful theoretical approaches are based on simulation methods known as quantum Monte Carlo (QMC) methods. Fermion systems are particularly challenging because no exact general simulation method is known which is able to treat systems containing more than a small number of fermions. This is because antisymmetry introduces minus signs into the sampling probabilities, the so-called fermion sign problem. The same techniques used to calculate correlated electronic systems, without the complication of the ionic background, can be applied to liquid ^{3}He. However, because liquid ^{3}He is more strongly correlated it is more challenging. As we will show in this paper, despite many years of research, the calculated helium equation of state and magnetic susceptibility is still in disagreement with experimental results.

QMC calculations of liquid helium began with work of McMillan [1] and Levesque *et al.* [2] who introduced the variational Monte Carlo method (VMC) and applied it to liquid ^{4}He. In 1974, Kalos *et al.* [3] performed the first exact simulation of hard-sphere bosons, an accurate model of liquid and solid helium using the Green's function Monte Carlo (GFMC) method. In 1977 Ceperley *et al.* [4] generalized the VMC method to many-fermion systems, and performed simulations of ^{3}He with the Slater–Jastrow (SJ) function. More accurate calculations [5] both within the fixed-node (FN) and release node procedure were developed for fermion systems in 1980 using the diffusion Monte Carlo scheme (DMC). Schmidt *et al.* [6] introduced backflow as well as 3-body correlations (BF-3B) into VMC and GFMC calculations of liquid ^{3}He. The first exact calculations by Lee *et al.* [7] using the transient estimate method established considerable error in the fixed-node results. Such calculations are only possible for quite small systems and full estimation of the convergence error is not possible. In 1995, Moroni *et al.* [8] determined more accurate optimized forms for the BF-3B wavefunction. Casulleras and Boronat (CB) [9] in 2000 revisited Panoff and Carlsons's [10] calculation with a newer potential as well as a re-optimized set of backflow parameters. Their results agree with experiments within statistical errors. Bouchaud and Lhuillier [11] using a pairing wavefunction obtained promising results for liquid ^{3}He but further calculations have yet to achieve energies as low as those obtained starting from a Fermi liquid trial function.

In addition to this theoretical motivation, there is considerable interest in understanding the properties of spin-polarized liquid ^{3}He. It is known that the superfluid state at very low temperatures is sensitive to an applied magnetic field [12]. It has been suggested that the critical temperature for the transition to the superfluid state will increase at strong fields. Experimental data for highly polarized liquid ^{3}He has been obtained [13] by sudden melting of solid ^{3}He.

Over 20 years ago, Levesque [14] applied VMC to polarized and unpolarized ^{3}He discovering the failure of VMC to predict the stability of the unpolarized state

*Author for correspondence. e-mail: ceperley@uiuc.edu

Molecular Physics ISSN 0026–8976 print/ISSN 1362–3028 online © 2003 Taylor & Francis Ltd
http://www.tandf.co.uk/journals
DOI: 10.1080/0026897031000085119

observed experimentally. With VMC using SJ trial functions, the fully polarized state has a lower energy than the unpolarized state at zero pressure, giving the wrong sign to the susceptibility. Even including 3-body correlation in the trial wave function, the Slater–Jastrow trial wavefunction could not achieve satisfactory agreement with experiments [14]. The incorrect prediction of spontaneous ferromagnetism in liquid ^{3}He had been earlier found by Manousakis *et al.* [15] using a many-body method based on hypernetted chain equations. They concluded that backflow is very important for a good energy at zero polarization but much less so for a fully polarized system. Using fixed-node DMC using plane wave nodal surfaces [16], the polarized state's energy was found to be slightly higher than the unpolarized state, but the susceptibility was still much too large. This behaviour can be easily understood because the wavefunction of fully polarized helium (with all helium spins lined up) is simpler than the unpolarized one and is easier to write down an accurate trial wavefunction. Thus there is more bias in the unpolarized energy.

One of the complications of assessing the progress in QMC calculations of liquid ^{3}He is that various computational methods, potentials and wavefunctions have been used over the years. In addition, since the actual interaction potential is not entirely due to 2-body interactions, corrections must be made for many-body electronic effects. It turns out that some of these complications have an energy scale of the same order of magnitude as the polarization energy, roughly $0.2\,\mathrm{K\,atom^{-1}}$. This paper reviews the current situation, reports the most accurate calculations with existing methods and potentials over a range of densities and polarizations, and corrects for the effect of the unknown many-body potential. We hope the assessment of the current state will spur improved fermion methods and calculations on this important physical system.

In the next section, we briefly introduce the effective potentials used in the calculation and estimate the effect of many-body terms in the interparticle interaction. We discuss the computational methods and procedures to correct for finite-size effects. Then, we show the result of our calculation of the liquid ^{3}He energy as a function of spin polarization.

2. Effective Hamiltonian

For a system of helium atoms at low densities and temperatures, the Born–Oppenheimer method is extremely accurate because the lowest lying electronic excitation is 230 000 K above the ground state. The resulting effective potential energy between the helium atoms is weak, dominated by a pair interaction and independent of the nuclear isotope. Our approach is to start with the best *ab initio* potential as determined by theoretical calculations. This potential has been recently tested for use with liquid ^{4}He and solid ^{3}He and ^{4}He systems, where the QMC 'sign problem' does not exist or is minimal. We then fit the small difference between the experimental and the theoretical equation of state by a polynomial and use this fit to estimate a correction to the potential. We consider an interaction potential of the form:

$$V(R) = \sum_{i<j} v_2(r_{ij}) + \sum_{i<j<k} v_3(\mathbf{r}_i, \mathbf{r}_j, \mathbf{r}_k) + \Delta E(\rho)N. \quad (1)$$

Here v_2 and v_3 are the 2 and 3-body potentials and $\Delta E(\rho)$ is the residual many-body potential, assumed to depend only on density.

Over the years, various forms of the two-body potential for helium atoms, obtained from empirical fitting to experimental data or *ab initio* calculations, have been proposed, giving better and better descriptions of helium interactions. We used the recent SAPT2 potential first developed by Korona *et al.* [17] and then refined by Janzen and Aziz [18] to consider the retardation effect in the dipole–dipole dispersion term as well as short distance behaviour. In addition to having all the correct theoretical behaviour, it also agrees with various experimental measurements of the He–He interaction, e.g. gas phase measurements.

The 3-body potential v_3 gives an important contribution to the total energy, although its precise form is not as well verified. We used the potential proposed by Cohen and Murrell (CM) [19], obtained by fitting to high quality *ab initio* data. In our simulation, the v_3 potential is treated perturbatively, i.e. the Monte Carlo sampling is determined by the two-body potential only and we add the 3-body contribution to the total energy by calculating the average $E_{3\mathrm{B}} = \langle v_3 \rangle$ over many-body helium configurations. At the densities of this study, the CM potential is dominated by the triple-dipole Axilrod–Teller interaction and is relatively smooth and much smaller in magnitude than the 2-body potential, justifying the use of the perturbation approach. The 3-body contribution does depend on helium density. We have verified that the variation of the 3-body potential with respect to ^{3}He polarization caused by the change in the local structure is at most $0.001\,\mathrm{K\,atom^{-1}}$. Note that the direct spin–spin interaction is extremely small in liquid ^{3}He. Converse to the positive contribution of CM potential, another form of the v_3, the well-known Bruch–McGee (BM) [20] potential is negative and not consistent with the experimental data [21].

Calculations [21] have shown that the SAPT2 potential with the CM 3-body term is capable of

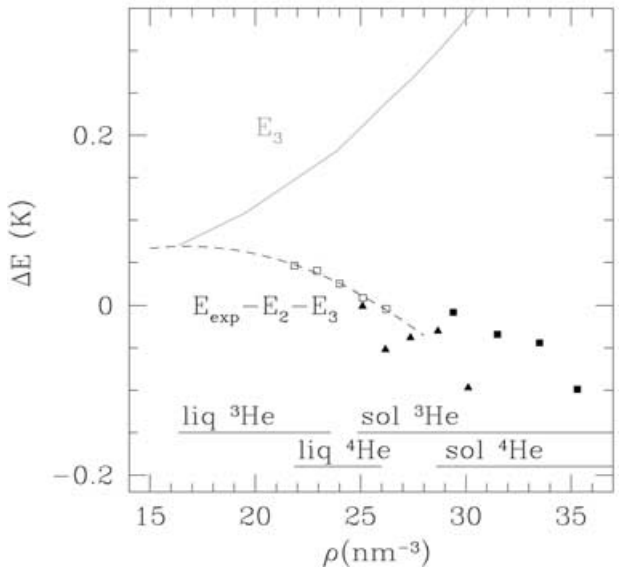

Figure 1. Our estimate of the 3-body CM potential for liquid and solid helium as a function of density (upper solid line). The symbols show the residual energy: the difference between the DMC computed 2-body + 3-body energy and experimental energies of solid ^{3}He and liquid and solid ^{4}He. The square points are ^{4}He, triangles are ^{3}He, solid points are crystal and open points are liquid. The dashed line is a quadratic fit to liquid ^{4}He. The density ranges of the various phases are shown on the bottom scale.

providing an accurate equation of state for solid ^{4}He as well as solid ^{3}He, provided the reference state for determining the equation of state (EOS) for ^{3}He is properly selected. Shown in figure 1 is the magnitude of the 3-body potential as a function of density and the difference between the computed 3-body potential and the experimental energy for the three phases for which QMC does not have a significant sign problem. As shown, the residual energy, ΔE is less than $0.10\,\mathrm{K\,atom^{-1}}$ and is roughly independent of density, phase and isotope. We then take the liquid ^{4}He residual energy and fit to a quadratic function in density to extrapolate to the density range of liquid ^{3}He. We note that in the density range: $21.58\ \mathrm{nm^{-3}} \leq \rho \leq 23.58\ \mathrm{nm^{-3}}$ both ^{3}He and ^{4}He are liquids, so extrapolation of the residual energy is unnecessary. The results are shown in table 1. We then add to the experimental ^{3}He energy versus density [12] our corrections from the 3-body potential and the residual energy to obtain an estimate of the ground state energy of a hypothetical ^{3}He liquid interacting solely with the 2-body SAPT2 potential. This is tabulated in table 1. We estimate the errors due to the extrapolation of the residual energy and of the ^{3}He experimental energy to be less than $0.01\,\mathrm{K\,atom^{-1}}$ at melting densities and $0.05\,\mathrm{K\,atom^{-1}}$ at zero pressure.

Table 1. Energies of liquid ^{3}He at the densities chosen for this study, in $\mathrm{K\,atom^{-1}}$. Density is in units of $\mathrm{atom\,nm^{-3}}$, E_{exp} is the experimental energy [22], $E_{3\mathrm{B}}$ is our estimate of the CM 3-body energy and ΔE is the residual energy extrapolated from liquid ^{4}He calculations [21]. $E_{2\mathrm{B}}$ is our estimate of the exact energy of a hypothetical Fermi liquid interacting with the SAPT2 potential. χ/C is the interpolated estimate of the magnetic susceptibility [23].

ρ	E_{exp}	$E_{3\mathrm{B}}$	ΔE	$E_{2\mathrm{B}}$	χ/C
16.35	−2.481	0.070	0.068	−2.619	2.82
19.46	−2.216	0.108	0.062	−2.386	3.86
23.80	−0.885	0.182	0.027	−1.094	5.90

To estimate the experimental magnetic equation of state, we use the magnetic susceptibility χ interpolated from experimental estimates [23] and shown in table 1, assuming a quadratic dependence of energy on polarization. There are recent measurements [24] finding that these values are too small by roughly 10%.

3. Methods

We use several quantum Monte Carlo methods. First variational Monte Carlo (VMC) is used to optimize parameters in trial wavefunctions. The trial wavefunction has two-body (Jastrow) 3-body and backflow correlations, shown [8] to provide essential improvements in liquid ^{3}He. We used an 11 parameter function (five parameters for the 2-body correlation, $u_2(r)$, three parameters for the three-body term, $\zeta(r)$ and three parameters for the backflow function $\eta(r)$). Calculations show that such a form is sufficient to achieve minimum energy and variance for this type of wavefunction. We use a combination of energy and variance optimization, with a full optimization of all of the wavefunction parameters at each density and polarization.

We then use diffusion Monte Carlo (DMC) with real wavefunctions (fixed node) or complex wavefunctions (fixed phase) to obtain a lower energy. This method gives the lowest upper bound consistent with the assumed fixed nodes or fixed phases. When extrapolated to the thermodynamic limit, the fixed node and fixed phase give the same upper bound if the same trial function was used. We used a DMC time step so that more than 99% trial moves are accepted giving a time step error of less than $0.005\,\mathrm{K\,atom^{-1}}$. As we show below, the assumption of the fixed nodes with nodes given by a backflow wavefunction dominates the other errors of the calculations and overestimates the exact energy by $\geq 0.25\,\mathrm{K\,atom^{-1}}$.

After the effect of the nodes, the dependence of the energy on the number of helium atoms is the largest systematic error. Usually one uses periodic boundary

conditions to reduce finite size effects. For Fermi liquids, there are sizable errors coming from the filling of shells in momentum space. These are typically corrected using Fermi liquid theory with an effective mass determined from VMC simulations with a variety of system sizes, done because DMC calculations with BF wavefunctions become quite lengthy for large N. However the correction done this way can have a systematic error if the size effect is different within VMC and DMC.

Here we employ twist averaged boundary conditions (TABC). Within periodic boundary conditions, the phase, picked up by the wavefunction as a particle makes a circuit across the unit cell, is arbitrary. General boundary conditions for a wavefunction are

$$\Psi(\mathbf{r}_1 + \mathbf{L}, \mathbf{r}_2, \ldots) = \exp(\mathrm{i}\theta)\Psi(\mathbf{r}_1, \mathbf{r}_2, \ldots), \tag{2}$$

where $\mathbf{L}$ is a lattice vector of the supercell. If the twist angle θ is averaged over, most single-particle finite-size effects, arising from shell effects in filling the plane wave orbitals, are eliminated. This is particularly advantageous for polarization calculations since shell effects dominate the polarization energy. The extra effort in integrating over the twist angles is minimal (we use a 10^3 grid), since the various calculations all serve to reduce the final variance of the computed properties. With this technique, one can calculate the energy versus polarization for systems with a fixed number of particles giving smooth curves of the polarization energy and much reduced systematic errors. The effect of boundary conditions is examined in detail in Lin *et al.* [25].

Another finite size effect comes from the truncation of the potential at the edge of the box. Since the 2-body potential extends beyond the range of the simulation cell we use a cutoff radius $\sigma = L/2$. The interatomic potential used in the DMC calculation is truncated and shifted:

$$\tilde{v}_2(r) = \begin{cases} v_2(r) - v_2(\sigma)\,, & r < \sigma, \\ 0, & r > \sigma, \end{cases} \tag{3}$$

We then correct for this truncation by adding the effect of the truncated potential evaluated within first-order perturbation theory. The 'tail' correction for the potential energy is

$$\delta V = 2\pi\rho \int_0^\infty r^2\, \mathrm{d}r g(r)[v_2(r) - \tilde{v}_2(r)]. \tag{4}$$

To perform the integral, the pair correlation function, $g(r)$ is extended from σ to much larger r by fitting the computed $g(r)$ and $S(k)$ to an assumed form [26] and integrating that form. These corrections are on the order of $0.018\,\mathrm{K\,atom^{-1}}$ at low pressure and $0.038\,\mathrm{K\,atom^{-1}}$ at high pressure for systems of 66 atoms.

The results of two different calculations, with different codes, one using TABC and the fixed-phase method and the other using PBC with Fermi-liquid theory size corrections and fixed nodes, both corrected for time-step errors, give the same result within $0.01\,\mathrm{K\,atom^{-1}}$, independent of the polarization. However, the TABC method allows one to have a more accurate calculation of the energy versus polarization since the necessity of extrapolation to large particle numbers is much reduced.

4. Comparison with previous calculations

We have difficulty comparing with many of the previous calculations because there have been a variety of integration algorithms, potentials, trial wavefunction, and size correction methods used. Taking account of these differences, the present calculations agree with those of Panoff and Carlson [10] and of Moroni *et al.* [8] within $0.01\,\mathrm{K\,atom^{-1}}$. There has been a recent claim by Casulleras and Boronat [9] (CB) that FN-DMC calculations are in agreement with experimental data to experimental precision. They used the HFD-B(HE) pair potential [27] and a backflow trial wavefunction, re-optimizing the backflow parameters and found a wavefunction with a fixed-node energy $E = -2.477(14)\,\mathrm{K\,atom^{-1}}$ at zero pressure. Agreement between the results of CB and the experimental equation of state extends throughout the range of liquid ^{3}He. As a test case, we used exactly the same potential, wavefunction and number of particles as used by CB, but we could not confirm their result. Our ground state energy is $E = -2.375\,\mathrm{K\,atom^{-1}}$, $0.10\,\mathrm{K\,atom^{-1}}$ higher than their result. As discussed above, the 2-body calculations should not be directly compared to experiment because of important three- and more-body terms in the bulk helium potential. We estimate that the true ground state energy for the HFD-B potential to be $-2.60\,\mathrm{K\,atom^{-1}}$, lower by $0.12\,\mathrm{K\,atom^{-1}}$ from their estimate. Although it is difficult to identify all the sources of the disagreement, we believe that differences in finite size-effect estimation are sizeable. The close agreement CB obtained with experiment is most likely a fortuitous cancellation of the finite size effects, the fixed-node error and the use of the HFD-B 2-body potential without correction for the many-body potential. The calculation, using their techniques, of the polarization energy as a function of density and the variational variance could help to resolve this disagreement.

5. Results

We performed calculations at three densities corresponding roughly to the maximum and minimum densities of liquid ^{3}He and to an intermediate density.

Table 2. Energy as a function of density and spin polarization in K atom^{-1}. Numbers in parenthesis are the statistical error (one standard deviation) in units of 10^{-4} K atom^{-1}. Results shown are obtained using twist-averaged boundary condition and corrected for potential size effects. The last column shows the intrinsic variance of the trial wavefunction in K^2 atom^{-1}.

ρ	ζ	E_{DMC}(K)	E_{VMC}	Variance
16.35	0.000	−2.3586(8)	−2.1633(9)	23
	0.242	−2.3548(10)	−2.1614(9)	18
	0.485	−2.3433(8)	−2.1753(9)	17
	0.727	−2.3270(8)	−2.1939(8)	14
	0.879	−2.2964(6)	−2.1904(7)	11
	1.000	−2.2544(8)	−2.1792(6)	10
19.46	0.000	−2.0685(13)	−1.7469(12)	30
	0.242	−2.0623(13)	−1.7499(12)	28
	0.485	−2.0807(11)	−1.7984(12)	28
	0.727	−2.0898(11)	−1.8599(10)	22
	0.879	−2.0777(9)	−1.8904(10)	19
	1.000	−2.0542(9)	−1.9088(8)	17
23.80	0.000	−0.6612(20)	−0.0184(20)	65
	0.242	−0.6619(21)	−0.0229(21)	54
	0.485	−0.6959(19)	−0.1358(20)	62
	0.727	−0.7480(18)	−0.2585(18)	48
	0.879	−0.7611(19)	−0.3336(17)	43
	1.000	−0.7579(17)	−0.4042(15)	40

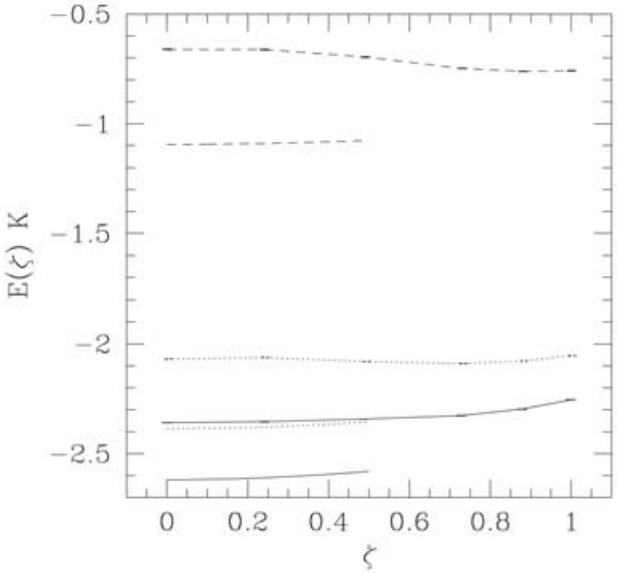

Figure 2. Computed energies of liquid ^{3}He using TA-DMC as a function of spin polarization. The three full length lines correspond to the three densities studied (increasing density corresponds to increasing energy) with the solid line 16.35 nm^{-3}, dotted line 19.46 nm^{-3} and dashed line 23.80 nm^{-3}. The lines extending from $0 \le \zeta \le 0.5$ show the estimated experimental energies corrected for the interactions beyond the pair potential with the polarization dependence using the zero-field susceptibility.

($\rho = 16.35$, 19.46 and 23.80 atoms nm^{-3}, corresponding to pressures equal to 0, 8.4 and 35.3 bar). At each density we did calculations at six different values of the spin polarization. The result of our calculations are given in table 2. The fixed-node error in the unpolarized energy varies from 0.26 K at zero pressure to 0.43 K at freezing density.

Figure 2 shows the spin polarization energy at the three densities. Also shown are the experimental estimates. The spin polarization energy of the experimental energies is an extrapolation from the magnetic susceptibilities in table 1. The magnetic susceptibility at low pressure is too small by a factor of 2 while at freezing density it predicts the polarized state is stable, in contradiction with experiment.

In figure 3 the result of TABC calculations at low density is shown. The dashed line is drawn assuming the helium magnetic susceptibility is constant at experimental $\zeta = 0$ value throughout the polarization range.

Figure 4 shows that the unpolarized trial wavefunction has a larger variance compared with the polarized one. This shows the quality of the polarized wavefunction is better and thus has a smaller bias. For DMC simulation, the error in the energy of the wavefunction is limited by the nodal structure. If one could improve the nodal description of liquid helium, we expect the energy of the unpolarized state to drop more than that of the

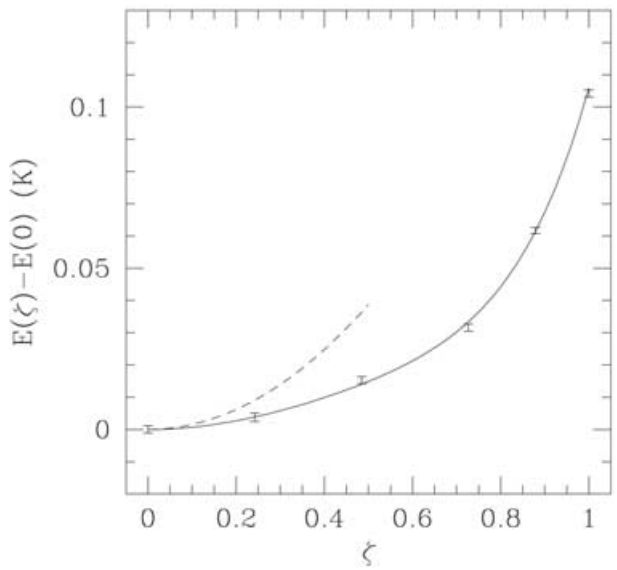

Figure 3. Energy versus polarization of liquid ^{3}He at $\rho = 16.35$ atom nm^{-3} with twist-averaged boundary conditions. The symbols are this calculation, the curve is a fit of the QMC data using a quadratic polynomial in ζ^2. The dashed line shows an extrapolation of the experimental data assuming $E = E_0 + \zeta^2/(2\chi/C)$.

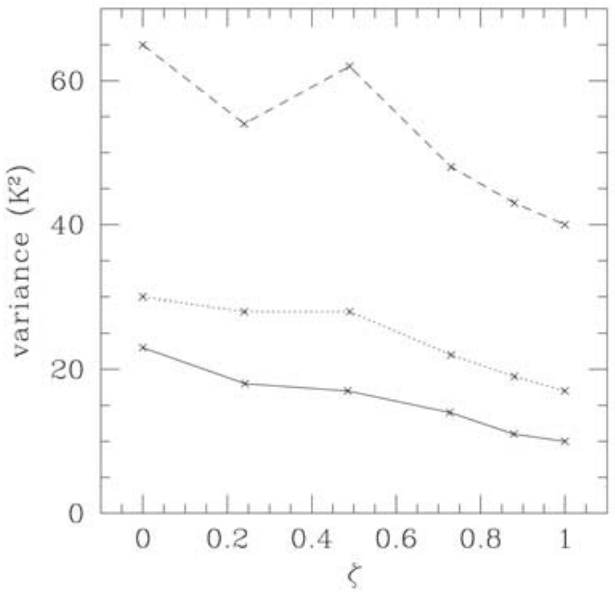

Figure 4. Variance versus spin polarization. The curves from the bottom to the top are at densities 16.35, 19.46 and 23.80 atom nm^{-3}.

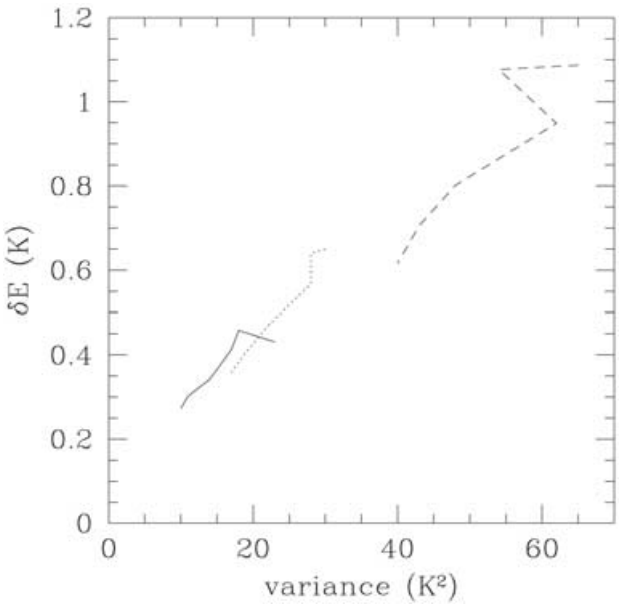

Figure 5. Variance versus the error of the variational energy with line styles as given in figure 2.

polarized state since there is more room for improvement of the unpolarized helium. As a result, the polarization energy curve will be closer to the experimental value. In the 3D electron gas the variance is roughly independent of the polarization [28].

Figure 5 shows how the variance correlates with the error in the variational energy, showing that the energy errors are as expected for wavefunctions of this quality.

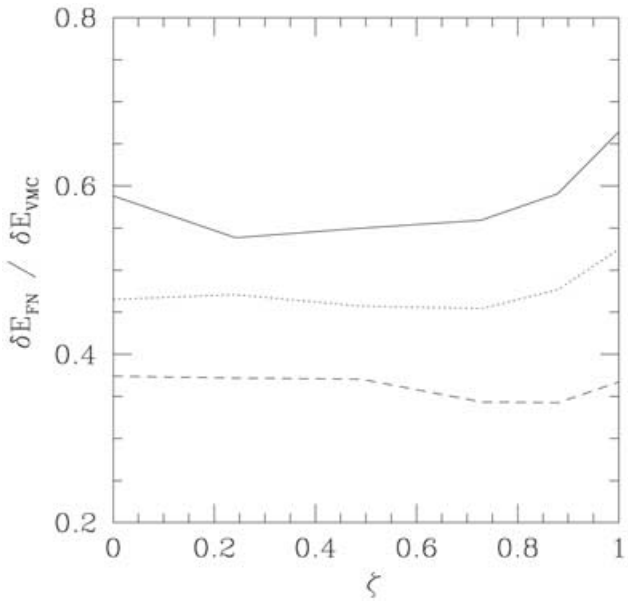

Figure 6. Error in energy in diffusion Monte Carlo relative to that in variational Monte Carlo using the same BF-3B trial function. Data from top to bottom correspond to densities of 16.35, 19.46 and 23.80 atom nm^{-3}.

In figure 6 it is shown how much the error is reduced in going from the variational result to the fixed-node result, with roughly 2/3 of the energy missing at high pressure but only 1/2 of the energy at low pressure being recovered using DMC. The nodal contributions are relatively more important at low density than at high density.

6. Conclusion

We calculated the polarization energy of liquid ^{3}He. It is harder to get the nodal surfaces correct for the unpolarized helium which causes a bias in the polarization energy curve. Because of the delicate cancellation (large susceptibility) this small error in energy turns into a big error in the susceptibility. The accurate calculation of helium polarization energy remains a challenge for quantum Monte Carlo. The errors appear larger than for corresponding calculations of electronic systems.

The question arises as to what terms will be needed to make a more accurate calculation. We have established that trial functions beyond the form considered here will be necessary. Comparison of the variational and fixed-node result show that the improvement has to come primarily from the Slater determinant. We have tried generalizing the 3B-BF trial function by letting the factors be spin-dependent and k-dependent and did not significantly lower the energy. Another possibility is to use a p-wave superfluid wavefunction, as was done in the work of Bouchaud and Lhuiller [11]. We only remark that the energies associated with pairing are

thought to be on the order of the transition temperature, namely ≈ 1 mK, which is several orders of magnitude smaller than the discrepancies we observe. We do not know how to improve the trial function to bring it closer to experimental results.

Other QMC methods can, in principle, achieve lower energies without improvement in the trial wavefunction. Exact fermion methods such as transient-estimate or released-node calculations [6] are quite feasible for small systems of 54 atoms but hard to improve upon the accuracy due to the fermion instability at long projection times. The exact fermion method of Kalos and Pederiva [29] will be useful in eliminating the fixed-node error, however, the method has only been applied to relatively small systems and scaling up to provide a definitive test remains to be done.

This research was supported by NSF DMR01-04399 and the Department of Physics at the University of Illinois Urbana-Champaign. Computational resources were provided by the NCSA.

References

[1] McMillan, W. C., 1965, *Phys. Rev.* A, **138,** 442.
[2] Levesque, D., Khiet, T., Schiff, D., and Verlet, L., 1965, Orsay report (unpublished).
[3] Kalos, M. H., Levesque, D., and Verlet, L., 1974, *Phys. Rev.* A, **9,** 2178.
[4] Ceperley, D., Chester, G. V., and Kalos, M. H., 1977, *Phys. Rev.* B, **16,** 3081.
[5] Ceperley, D. M., and Alder, B. J., 1980, *Phys. Rev. Lett.*, **45,** 566.
[6] Schmidt, K. E., Lee, M. A., Kalos, M. H., and Chester, G. V., 1981, *Phys. Rev. Lett.*, **47,** 807.
[7] Lee, M. A., Schmidt, K. E., Kalos, M. H., and Chester, G. V., 1981, *Phys. Rev. Lett.*, **46,** 728.
[8] Moroni, S., Fantoni, S., and Senatore, G., 1995, *Phys. Rev.* B, **52,** 13547.
[9] Casulleras, J., and Boronat, J., 2000, *Phys. Rev. Lett.*, **84,** 3121.
[10] Panoff, R. M., and Carlson, J., 1989, *Phys. Rev. Lett.*, **62,** 1130.
[11] Bouchaud, J. P., and Lhuillier, C., 1988, *Spin Polarized Quantum Systems*, edited by S. Stringari (Singapore: World Scientific).
[12] Wheatley, J. C., 1975, *Rev. mod. Phys.*, **47,** 415.
[13] Wiegers, S. A. J., Wolf, P. E., and Puech, L., 1991, *Phys. Rev. Lett.*, **66,** 2895.
[14] Levesque, D., 1980, *Phys. Rev.*, **21,** 5159; 1981, *Phys. Rev.* B, **23,** 2203.
[15] Manousakis, E., Fantoni, S., Pandharipande, V. R., and Usmani, Q. N., 1983, *Phys. Rev.* B, **28,** 3770.
[16] Ceperley, D. M., 1995, *The Proceedings of the Les Houches Summer School, Session 56, Strongly Interacting Fermions and High T_c Superconductivity*, edited by B. Doucot and J. Zinn-Justin (Amsterdam: Elsevier), p. 427.
[17] Korona, T., Williams, H. L., Bukowski, R., Jeziorski, B., and Szakewicz, K., 1997, *J. chem. Phys.*, **106,** 5109.
[18] Janzen, A. R., and Aziz, R. A., 1997, *J. chem. Phys.*, **107,** 914.
[19] Cohen, M. J., and Murrell, J. N., 1996, *Chem. Phys. Lett.*, **260,** 371.
[20] Bruch, L. W., and McGee, I. J., 1973, *J. chem. Phys.*, **59,** 409.
[21] Moroni, S., Pederiva, F., Fantoni, S., and Boninsegni, M., 2000, *Phys. Rev. Lett.*, **84,** 2650.
[22] Aziz, R. A., and Pathria, R. K., 1973, *Phys. Rev.* A, **7,** 809; The energy at zero pressure is from Reesink, L., 2001, PhD thesis, University of Leiden, Germany.
[23] Ramm, H., Pedroni, P., Thompson, J. R., and Meyer, H., 1970, *J. low temp. Phys.*, **2,** 539.
[24] Triqueneaux, S., 2001, PhD thesis, University of Toulouse and CNRS-CRTBT Grenoble, France; Godfrin, H., 2002, *Introduction to Modern Methods of Quantum Many-Body Theory and their Applications, Series Advances in Quantum Many-body Theories*, Vol. 7, edited by A. Fabrocini, S. Fantoni and E. Krotscheck (Singapore: World Scientific), p. 329.
[25] Lin, C., Zong, F.-H., and Ceperley, D. M., 2001, *Phys. Rev.* E, **64,** 016702.
[26] Ceperley, D. M., and Chester, G. V., 1977, *Phys. Rev.* A, **15,** 755.
[27] Aziz, R. A., McCourt, F. R. W., and Wong, C. C. K., 1987, *Molec. Phys.*, **61,** 1487.
[28] Zong, F. H., Lin, C., and Ceperley, D. M., 2002, *Phys. Rev.* E, **66,** 036703:1-7.
[29] Kalos, M. H., and Pederiva, F., 2000, *Phys. Rev. Lett.*, **85,** 3547.